

DOUBLY HEAVY EXOTIC MESONS AND BARYONS AND HOW TO LOOK FOR THEM*

MAREK KARLINER

Raymond and Beverly Sackler School of Physics and Astronomy
Tel Aviv University, Tel Aviv, Israel
marek@proton.tau.ac.il

(Received December 6, 2015)

I discuss the experimental evidence for and theoretical interpretation of the new mesons and baryons with two heavy quarks. These include doubly-heavy baryons, exotic hadronic quarkonia and, most recently, a manifestly exotic pentaquark-like doubly heavy baryon discovered by LHCb with a minimal quark content $uud\bar{c}$. Its mass, decay mode and width are in agreement with a prediction based on a physical picture of a deuteron-like $\Sigma_c\bar{D}^*$ “hadronic molecule”. In the second part of the paper, I focus on possible ways of experimental exploration of this new spectroscopy of QCD, especially in future high-energy e^+e^- colliders with very high luminosity. The primary task of these machines is searching for physics beyond the Standard Model. Consequently, their planned CM energy is far above the relevant energy scale for production of the new doubly-heavy hadrons. Yet, preliminary analysis of radiative-return processes indicates rather high effective luminosity at CM energies of interest, suggesting a possibility for copious production.

DOI:10.5506/APhysPolB.47.117

1. First observation of manifestly exotic hadrons

In late 2007, the Belle Collaboration reported [1] anomalously large rate partial widths of $\Upsilon(5S) \rightarrow \Upsilon(2S)$ and $\Upsilon(5S) \rightarrow \Upsilon(1S)$, two orders of magnitude larger than the analogous decays of $\Upsilon(3S)$. Soon afterwards, Lipkin and I proposed [2] that a four-quark exotic resonance $[b\bar{b}u\bar{d}]$ might mediate these decays through the cascade $\Upsilon(mS) \rightarrow [b\bar{b}u\bar{d}]\pi^- \rightarrow \Upsilon(nS)\pi^+\pi^-$. We suggested looking for the $[b\bar{b}u\bar{d}]$ resonance in these decays as peaks in the invariant mass of $\Upsilon(1S)\pi$ or $\Upsilon(2S)\pi$ systems, *cf.* Fig. 1. More recently, the Belle Collaboration confirmed this prediction, announcing [3, 4] the obser-

* Presented at the LV Cracow School of Theoretical Physics “Particles and Resonances of the Standard Model and Beyond”, Zakopane, Poland, June 20–28, 2015.

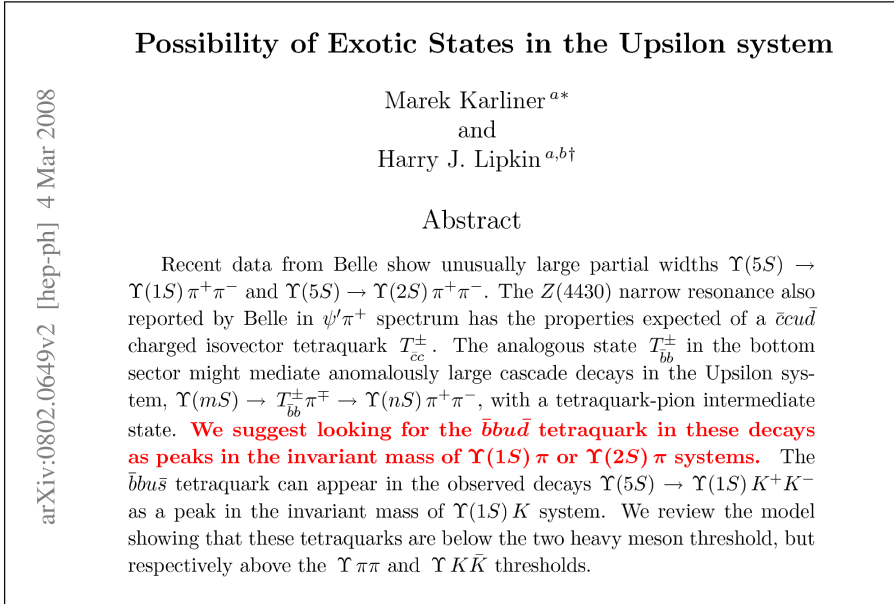


Fig. 1. First page of our paper [2] proposing a four-quark exotic intermediate state $\bar{b}b u \bar{d}$ as an explanation of the anomalously large rate partial widths of $\Upsilon(5S) \rightarrow \Upsilon(2S)$ and $\Upsilon(5S) \rightarrow \Upsilon(1S)$.

vation of two charged bottomonium-like resonances Z_b as narrow structures in $\pi^\pm \Upsilon(nS)$ ($n = 1, 2, 3$) and $\pi^\pm h_b(mP)$ ($m = 1, 2$) mass spectra that are produced in association with a single charged pion in $\Upsilon(5S)$ decays. The measured masses of the two structures averaged over the five final states are $M_1 = 10608.4 \pm 2.0$ MeV, $M_2 = 10653.2 \pm 1.5$ MeV, both with a width of about 15 MeV. Interestingly enough, the two masses M_1 and M_2 are about 3 MeV above the respective $B^* \bar{B}$ and $B^* \bar{B}^*$ thresholds.

This strongly suggests a parallel with $X(3872)$, whose mass is almost exactly at the $D^* \bar{D}$ threshold. It also raises the possibility that such states might have a complementary description as deuteron-like “molecule” of two heavy mesons quasi-bound by pion exchange [5–7], as schematically shown in figure 2.

The attraction due to π exchange is 3 times weaker in the $I = 1$ channel than in the $I = 0$ channel. Consequently, in the charm system, the $I = 1$ state is expected to be well above the $D^* \bar{D}$ threshold and the $I = 0$ $X(3872)$ is at the threshold¹. In the bottom system, the attraction due to π exchange

¹ For simplicity, we treat $X(3872)$ as an isoscalar, since it has no charged partners, and we ignore here the issue of isospin breaking in its decays. A more refined treatment results in the same conclusions.



Fig. 2. Diagrams contributing to $B\bar{B}^*$ and $B^*\bar{B}^*$ binding through pion exchange. Analogous diagrams contribute to $D\bar{D}^*$ and $D^*\bar{D}^*$ binding, modulo the caveat that $D^* \rightarrow D\pi$, while $B^* \rightarrow B\pi$ is kinematically forbidden, as discussed in the text.

is essentially the same, but the kinetic energy is much smaller by a factor of $\sim m(B)/m(D) \approx 2.8$. Therefore, the net binding is much stronger than in the charm system.

The recently discovered manifestly exotic charged resonances are surprisingly narrow. This is the case in both $\bar{b}b$ systems [3, 4] — and in the exotic charmonium, namely the remarkable peak $Z_c(3900)$ at $3899.0 \pm 3.6 \pm 4.9$ MeV with $\Gamma = 46 \pm 10 \pm 20$ MeV reported by BESIII [8].

The relatively slow decay of these exotic resonances implies that the dominant configuration of the $\bar{Q}Q\bar{q}q$ four-body system is *not* that of a low-lying $\bar{Q}Q$ quarkonium and pion(s). The latter have a much lower energy than the respective two-meson thresholds $\bar{M}M^*$ and \bar{M}^*M^* , ($M = D, B$), but do readily fall apart into $(\bar{Q}Q)$ and pion(s) and would result in very large decay widths. We should view these systems as loosely bound states and/or near threshold resonances in the two heavy-meson system.

Such “molecular” states, $\bar{D}D^*$, *etc.*, were introduced in Ref. [5]. They were later extensively discussed [6, 7] in analogy with the deuteron which binds via exchange of pions and other light mesons, and were referred to as *deusons*. The key observation is that the coupling to the heavy mesons of the light mesons exchanged (π, ρ , *etc.*) becomes universal and independent of M_Q for $M_Q \rightarrow \infty$, and so does the resulting potential in any given J^{CP} and isospin channel. In this limit, the kinetic energy $\sim p^2/(M_Q)$ vanishes, and the two heavy mesons bind with a binding energy \sim the maximal depth of the attractive meson-exchange potential.

For a long time, it has been an important open question whether these considerations apply in the real world with large but finite masses of the D and B mesons. The recent experimental results of Belle [3, 4] and BESIII [8], together with the theoretical analysis in Refs. [9] and [10] strongly indicate that such exotic states do exist — some were already found and more are predicted below.

Due to parity conservation, the pion cannot be exchanged in the $\bar{M}M$ system, but it does contribute in the $\bar{M}M^*$ and \bar{M}^*M^* channels. The $\vec{\tau}_1 \cdot \vec{\tau}_s$ isospin nature of the exchange implies that the binding is 3 times stronger in the isoscalar channel. It was estimated [9, 10] that in the bottomonium system, this difference in the binding potentials raises the $I = 1$ exotics well above the $I = 0$ exotics. In the charmonium system, this splitting is expected to be slightly smaller, because the $\bar{D}D^*/\bar{D}^*D^*$ states are larger than $\bar{B}B^*/\bar{B}^*B^*$. This is because the reduced mass in the $\bar{B}B^*$ system is approximately 2.5 times larger than in the $\bar{D}D^*$ system. On the other hand, the net attractive potential due to the light mesons exchanged between the heavy-light mesons is approximately the same, since $m_c, m_b \gg \Lambda_{\text{QCD}}$. As usual in quantum mechanics, for a given potential, the radius of a bound state or a resonance gets smaller when the reduced mass grows, so the $\bar{D}D^*$ states are larger than the $\bar{B}B^*$ states. Because of this difference in size, the attraction in both $I = 0$ and $I = 1$ charmonium channels is expected to be somewhat smaller.

Since the quarks are heavy, we can treat their kinetic energy as a perturbation depending linearly on a parameter inversely proportional to μ_{red} , the reduced mass of the two meson system, which scales like the mass of the heavy quark [11], with the Hamiltonian $H = ap^2 + V$, where $a = 1/\mu_{\text{red}} \sim 1/m_Q$. We can use the existing data in order to make a very rough estimate of the isovector binding potential in the $m_Q \rightarrow \infty$ limit. We have two data points: $Z_c(3900)$ at $a(D)$ is approximately 27 MeV above $\bar{D}D^*$ threshold and $Z_b(10610)$ at $a(B)$ is approximately 3 MeV above $\bar{B}B^*$ threshold. Linear extrapolation to $a = 0$ yields $E_b^{I=1}(a = 0) \approx -11.7$ MeV. In view of the convexity, the actual binding energy is likely to slightly exceed this linear extrapolation.

We can then use this result for the isovector channel to estimate the $\bar{B}B^*$ binding in the isoscalar channel assuming that the isoscalar binding energy in the $m_Q \rightarrow \infty$ limit is 3 times larger than for the isovector, *i.e.* $E_b^{I=0}(a = 0) \approx 3 \times (-11.7) = -35$ MeV. $X(3872)$ is at $\bar{D}D^*$ threshold, providing an additional data point of $E_b^{I=0}(a(D)) \approx 0$ in the isoscalar channel. Linear extrapolation to $a(B)$ yields approximately -20 MeV as the $\bar{B}B^*$ binding energy in the isoscalar channel.

The upshot is that the $Z_c(3900)$ isovector resonance confirms and refines the estimates in [9, 10] for the mass of the putative $\bar{B}B^*$ isoscalar bound state. This immediately leads to several predictions [11]:

- (a) two $I = 0$ narrow resonances X_b in the bottomonium system, about 23 MeV below $Z_b(106010)$ and $Z_b(10650)$, *i.e.* about 20 MeV below the corresponding $\bar{B}B^*$ and \bar{B}^*B^* thresholds;
- (b) an $I = 1$ resonance above \bar{D}^*D^* threshold;
- (c) an $I = 0$ resonance near \bar{D}^*D^* threshold.

More recently, the BESIII Collaboration reported observation in $e^+e^- \rightarrow (D^*\bar{D}^*)^\pm\pi^\mp$ of what looks just like (b) above, namely a new charmonium-like charged resonance $Z_c(4025)$, slightly above the \bar{D}^*D^* threshold, at $\sqrt{s} = (4026.3 \pm 2.6 \pm 3.7)$ MeV, with width of $24.8 \pm 5.6 \pm 7.7$ MeV [12]. Shortly afterward, BESIII reported observation of another charged charmonium-like structure $Z_c(4020)$ in $e^+e^- \rightarrow \pi^+\pi^-h_c$ at $(4022.9 \pm 0.8 \pm 2.7)$ MeV and width of $7.9 \pm 2.7 \pm 2.6$ MeV [13]. At this time, it is not yet clear if these are two independent resonances or two observations of the same object at slightly different masses, possibly due to systematic effects associated with the two observation channels.

Figures 3 and 4 provide a concise summary of the experimental information about the masses of doubly-heavy exotics observed so far, together with our predictions for additional states, as discussed above.

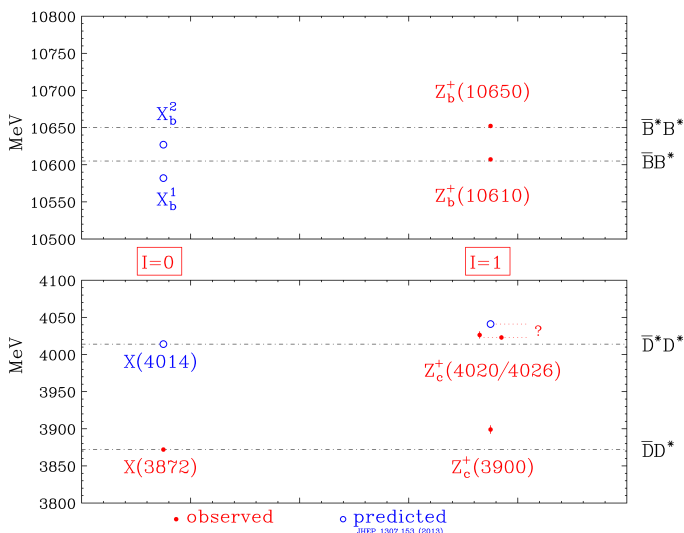


Fig. 3. Masses of the doubly-heavy exotic quarkonia *vs.* two-meson thresholds. The states observed so far are shown in gray/red, the predicted states are shown in black/blue. $I = 0$ resonances are shown on the left and isovectors are shown on the right. Note the proximity of all the states to the corresponding two-meson thresholds.

It is somewhat puzzling that, unlike $Z_c^+(3900)$, $Z_c^+(4020/4026)$ has not been seen in the $J/\psi\pi^+$ mode. Moreover, one notes that $Z_c^+(4020/4026)$ is somewhat closer to the \bar{D}^*D^* threshold than our prediction. It will be interesting to identify the reasons for this small difference. The two main possibilities are: (a) details of the experimental analysis; (b) a possible difference between the \bar{B}^*B^* and \bar{D}^*D^* attractive pion-exchange potentials.

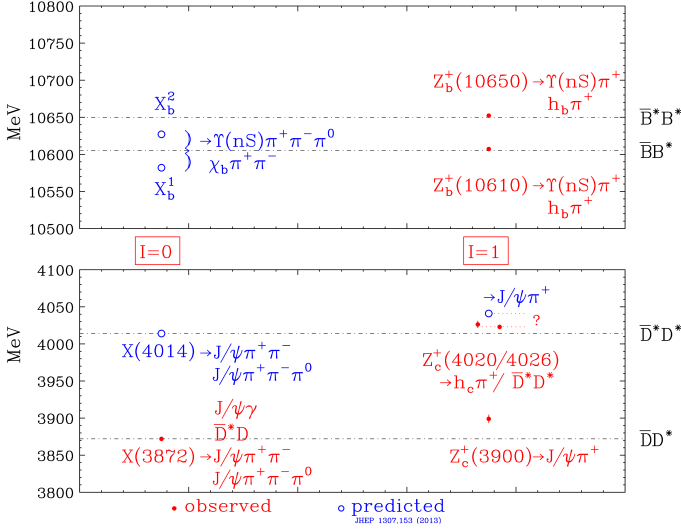


Fig. 4. Decay channels of doubly-heavy exotic quarkonia. The legend is as in figure 3.

Such a difference might perhaps be due to the fact that $m(B^*) - [m(B) + m(\pi)] \approx -94$ MeV, while $m(D^*) - [m(D) + m(\pi)] \approx 0^\pm$, depending on the D^* and π charges, affecting energy denominators in virtual pion emission.

The X_b states can most likely be observed through the decays $X_b \rightarrow \Upsilon\omega$ or $X_b \rightarrow \chi_b\pi\pi$. Unlike incorrectly stated in [11], they *cannot* decay to $\Upsilon\pi\pi$. The latter decays are prevented by G -parity conservation [14]. The observed decay $X(3872) \rightarrow J/\psi\pi\pi$ is only possible because isospin is strongly broken between D^+ and D^0 , and because $X(3872)$ is at the $\bar{D}D^*$ threshold. In contradistinction, in the bottomonium system isospin is almost perfectly conserved. *Thus the null result in CMS search [15] for $X_b \rightarrow \Upsilon(1S)\pi^+\pi^-$ does not tell us if X_b exists.* In fact, as we shall see next, X_b might have been already observed, camouflaging as run-of-the-mill excited bottomonium.

1.1. X_b as mixture of $\bar{B}B^*(1^{++})$ and $\chi_b(3P)$

The measured value of the radiative decays

$$R_{\psi\gamma} \equiv \frac{\mathcal{B}(X(3872) \rightarrow \psi(2S)\gamma)}{\mathcal{B}(X(3872) \rightarrow J/\psi\gamma)} = 2.46 \pm 0.64 \pm 0.29 \text{ [LHCb]} \quad (1)$$

suggests that $X(3872)$ is a mixture of $\chi_{c1}(2P)$ and $D^0\bar{D}^{*0}$.

We expect a similar mixing in the bottomonium system, with a slight twist: $\chi_{b1}(2P)$ is much too light, but $\chi_{b1}(3P)$ is near the expected X_b mass. It has been seen in $\chi_{b1}(3P) \rightarrow \Upsilon(mS)\gamma$, $m = 1, 2, 3$, by ATLAS, D0 and LHCb.

X_b and $\chi_{1b}(3P)$ have the same quantum numbers and their masses are expected to be close (*cf.* Table I and Fig. 5), so mixing between them is inevitable. We therefore conclude that X_b might have been seen already, by ATLAS, D0 and LHCb, camouflaging as $\chi_{1b}(3P)$ [20].

TABLE I

Values of $M(\chi_{b1}(3P))$ observed in various experiments.

Collaboration	Reference	Value [MeV/ c^2]
ATLAS	[16]	$10530 \pm 5 \pm 9$
D0	[17]	$10551 \pm 14 \pm 17$
LHCb (a)	[18]	$10511.3 \pm 1.7 \pm 2.5$
LHCb (b)	[19]	$10515.7^{+2.2+1.5}_{-3.9-2.1}$

(a) Using non-converted photons. (b) Using converted photons.

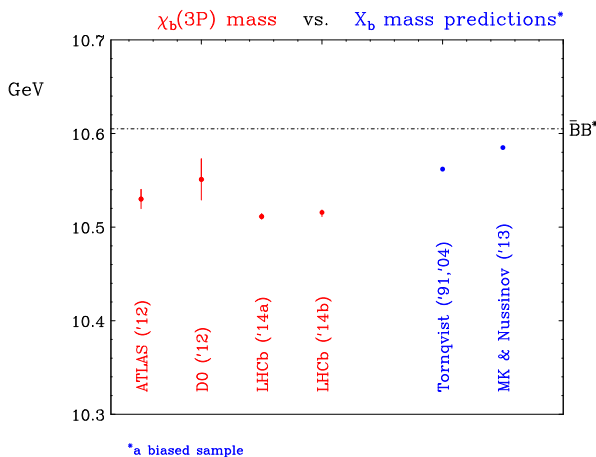


Fig. 5. Comparison of measured values of $\chi_{b1}(3P)$ mass with predicted values of X_b mass.

When discussing molecular states (of which $X(3872)$ is at least a partial example), one notices that narrow resonances have been discovered very close to $\bar{D}D^*$, \bar{D}^*D^* and $\bar{B}B^*$, \bar{B}^*B^* thresholds, but no analogous resonances have been observed close to $\bar{D}D$ or $\bar{B}B$ threshold; *cf.* Table II. The absence of narrow resonances at $\bar{D}D$ and $\bar{B}B$ thresholds provides a strong hint that forces such as pion exchange play a role in the formation of these resonances, because one-pion exchange cannot bind two pseudoscalars. Moreover, the heavy-light mesons D , D^* , B and B^* contain only one light quark, so their coupling to pions is significantly smaller than $g_{\pi NN}$. Therefore, in molecular systems containing two heavy-light mesons two-pion exchange is suppressed in comparison with one-pion exchange.

TABLE II

Five narrow exotic states close to meson–meson thresholds.

State	Mass ^a [MeV]	Width ^a [MeV]	$\bar{Q}Q$ decay mode	Phase space ^b [MeV]	Nearby threshold	ΔE [MeV]
$X(3872)$	3872	< 1.2	$J/\psi \pi^+ \pi^-$	495	$\bar{D}D^*$	< 1
$Z_b(10610)$	10608	21	$\Upsilon\pi$	1008	$\bar{B}B^*$	2 ± 2
$Z_b(10650)$	10651	10	$\Upsilon\pi$	1051	\bar{B}^*B^*	2 ± 2
$Z_c(3900)$	3900	24–46	$J/\psi \pi$	663	$\bar{D}D^*$	24
$Z_c(4020)$	4020	8–25	$J/\psi \pi$	783	\bar{D}^*D^*	6
\times					$\bar{D}D$	
\times					$\bar{B}B$	

^aMasses and widths approximate.^bQuarkonium decay modes listed have maximum phase space.

Strong support for the molecular interpretation of the states listed in Table II comes from the fact that they are quite narrow, despite many hundreds of MeV available for their decay into quarkonium and pion(s). The width is a product of the available (very large) phase space and the square of the absolute value of the matrix element between the initial and the final state. Thus, the experiments tell us that the overlap of the resonance wave function with quarkonium must be very small. In a tightly-bound pentaquark, the c and \bar{c} quarks are both within one confinement volume, so the overlap with the J/ψ wave function is then generically large. On the other hand, in the molecular picture, such a small overlap of the wave functions is automatic. This is because in a hadronic molecule, the two heavy quarks spend most of their time far from each other. This point is schematically illustrated in Fig. 6.

One then can infer from Table II the *necessary* conditions for existence of a near-threshold resonance of this type:

- (a) The state contains two heavy hadrons. They have to be heavy, as the repulsive kinetic energy is inversely proportional to the reduced mass.
- (b) The two hadrons carry isospin, so that they can couple to pions. Channels like $\Sigma_c \bar{\Lambda}_c$, in which one of the particles has zero isospin, can exchange a pion to become the equal-mass channel $\Lambda_c \bar{\Sigma}_c$.
- (c) The spin and parity of the two hadrons have to be such that they can bind through single pion exchange.
- (d) The hadrons making up the molecule have to be sufficiently narrow, as the molecule's width cannot be smaller than the sum of its constituents' widths.

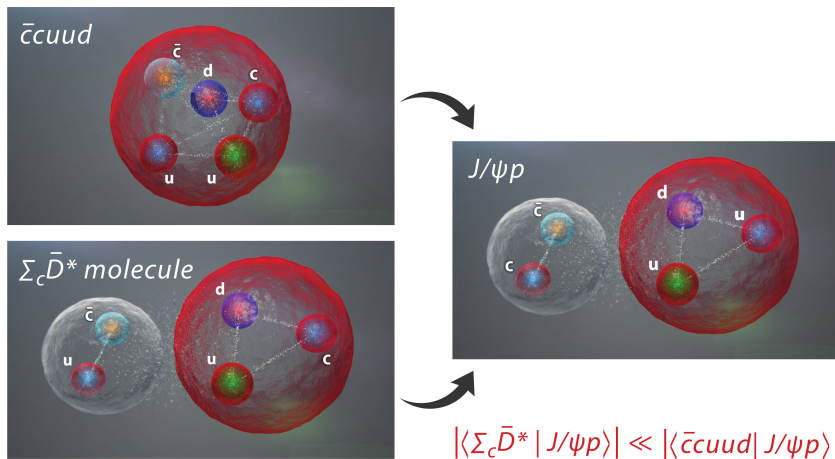


Fig. 6. Schematic comparison of decay of a tightly-bound pentaquark *vs.* hadronic molecule into $J/\psi p$. The overlap of the hadronic molecule wave function with the $J/\psi p$ final state is generically much smaller than for a tightly-bound pentaquark.

A crucial step is then the realization that *the pion-exchange binding mechanism can, in principle, apply to any two heavy hadrons which satisfy conditions (a)–(d) above, be they mesons or baryons.*

A quantitative understanding of these effects can be then applied to bound or resonant states of two heavy hadrons. For example, the discovery of the Z_b states and their probable interpretation as $B^* \bar{B}$ and $B^* \bar{B}^*$ bound by pion exchange led us to propose that a weakly bound $\Sigma_c \bar{D}^*$ deuteron-like state might exist [21]. The narrow pentaquark resonance discovered by LHCb [22] has the right properties to be that state. Many more analogous loosely bound states of two heavy hadrons are predicted [21]. They are listed in Table III. Note, in particular, the bottom quark analogue of the resonance discovered by LHCb [22], expected somewhat below the $\Sigma_b B^*$ threshold at 11140 MeV. Note also that in the open flavor sector, we expect a $D^* B^*$ resonance, but no DB^* . This is because a bound state of a pseudoscalar and a vector of different flavors cannot bind by one pion exchange.

1.2. A $(\Sigma_b^+ \Sigma_b^-)$ beauteron dibaryon?

In addition to the states listed in Table III, there is an interesting possibility of genuine dibaryons, *e.g.* a *strongly bound* $\Sigma_b^+ \Sigma_b^-$, $\Sigma_b^\pm \Sigma_c^\mp$ and $\Sigma_c^+ \Sigma_c^-$ *deuteron-like states* [23]. The Σ_b is about 500 MeV heavier than B^* . The $\Sigma_b \Sigma_b$ kinetic energy is therefore significantly smaller than that of $B \bar{B}^*$ or $B^* \bar{B}^*$. Moreover, Σ_b with $I = 1$ couples more strongly to pions than B and B^* with $\frac{I=1}{2}$. The opposite electric charges of Σ_b^+ and Σ_b^- provide additional

TABLE III

Thresholds for $Q\bar{Q}'$ doubly-heavy molecular states.

Channel	Minimum isospin	Minimal quark content ^{a,b}	Threshold [MeV] ^c	Example of decay mode
$D\bar{D}^*$	0	$c\bar{c}q\bar{q}$	3875.8	$J/\psi \pi\pi$
$D^*\bar{D}$	0	$c\bar{c}q\bar{q}$	4017.2	$J/\psi \pi\pi$
D^*B^*	0	$c\bar{b}q\bar{q}$	7333.8	$B_c^+ \pi\pi$
$\bar{B}B^*$	0	$b\bar{b}q\bar{q}$	10604.6	$\Upsilon(nS)\pi\pi$
\bar{B}^*B	0	$b\bar{b}q\bar{q}$	10650.4	$\Upsilon(nS)\pi\pi$
$\Sigma_c\bar{D}^*$	1/2	$c\bar{c}qqq'$	4462.4	$J/\psi p$
$\Sigma_c B^*$	1/2	$c\bar{b}qqq'$	7779.5	$B_c^+ p$
$\Sigma_b\bar{D}^*$	1/2	$b\bar{c}qqq'$	7823.0	$B_c^- p$
$\Sigma_b B^*$	1/2	$b\bar{b}qqq'$	11139.6	$\Upsilon(nS)p$
$\Sigma_c\bar{\Lambda}_c$	1	$c\bar{c}qq'\bar{u}\bar{d}$	4740.3	$J/\psi \pi$
$\Sigma_c\bar{\Sigma}_c$	0	$c\bar{c}qq'\bar{q}\bar{q}'$	4907.6	$J/\psi \pi\pi$
$\Sigma_c\bar{\Lambda}_b$	1	$c\bar{b}qq'\bar{u}\bar{d}$	8073.3 ^d	$B_c^+ \pi$
$\Sigma_b\bar{\Lambda}_c$	1	$b\bar{c}qq'\bar{u}\bar{d}$	8100.9 ^d	$B_c^- \pi$
$\Sigma_b\bar{\Lambda}_b$	1	$b\bar{b}qq'\bar{u}\bar{d}$	11433.9	$\Upsilon(nS)\pi$
$\Sigma_b\bar{\Sigma}_b$	0	$b\bar{b}qq'\bar{q}\bar{q}'$	11628.8	$\Upsilon(nS)\pi\pi$

^aIgnoring annihilation of quarks. ^bPlus other charge states when $I \neq 0$.^cBased on isospin-averaged masses. ^dThresholds differ by 27.6 MeV.

2–3 MeV of binding energy. Analogous considerations apply to $\Sigma_b^\pm \Sigma_c^\mp$ and $\Sigma_c^+ \Sigma_c^-$ states. The heavy dibaryon bound state might be sufficiently long-lived to be observed experimentally. A possible decay mode of the beauteron is $(\Sigma_b^+ \Sigma_b^-) \rightarrow \Lambda_b \Lambda_b \pi^+ \pi^-$, which might be observable in LHCb. It should also be seen in lattice QCD.

2. $QQ\bar{q}\bar{q}$ tetraquarks

The quark content of the exotic resonances observed so far is $\bar{Q}Qq\bar{q}$. A very different type of exotics are the $QQ\bar{q}_1\bar{q}_2$ tetraquarks (TQ-s) [24–27]. If such states do exist, producing and discovering even the lightest $cc\bar{u}\bar{d}$ is an extraordinary challenge. One needs to produce *two* $\bar{Q}Q$ pairs and then rearrange them, so as to form QQ and $\bar{Q}\bar{Q}$ diquarks, rather than the more favorable configuration of two $\bar{Q}Q$ and color singlets. *Then*, the QQ diquark needs to pick up a $\bar{u}\bar{d}$ light diquark, rather than a q , to make a QQq baryon, suppressing the production rate of these TQ-s below the rate of QQq production.

Yet, as discussed below, there are reasons for optimism. Observation of the doubly-heavy $B_c = (\bar{b}c)$ mesons [28] suggests that simultaneous production of $\bar{b}b$ and $\bar{c}c$ pairs which are close to each other in space and in rapidity and can coalesce to form doubly-heavy hadrons is not too rare. As discussed in detail in the next section, this is an encouraging sign for the prospects of producing and observing the ccq and bcs baryons and hopefully also the $cc\bar{u}\bar{d}$ TQ. ATLAS and CMS and especially LHCb probably have the best chance of discovering these states. If the new TQ lies below say, the DD^* threshold, it will be stable under the strong interaction and will decay only weakly.

Once the mass of the doubly heavy baryons is known, one can immediately estimate the mass of the corresponding tetraquark [11, 26] and check whether or not it is below the two B meson threshold

$$m(bb\bar{u}\bar{d}) = m(\Xi_{bbu}) + m(\Lambda_b) - m(B^0) - \frac{1}{4}[m(B^*) - m(B)]. \quad (2)$$

3. Doubly-heavy baryons

From the point of view of QCD, there is nothing exotic about baryons containing two heavy quarks (b or c , generically denoted by Q) and one light quark (u or d , generically denoted by q). Heavy quarks decay only by weak interaction, with a characteristic lifetime orders of magnitude larger than the typical QCD timescale, so from the point of view of strong interactions, the QQq baryons are stable, just like protons, neutrons and hyperons. Thus, these *doubly-heavy* baryons *must* exist.

On the other hand, producing and discovering them is an extraordinary challenge. One needs to produce *two* $\bar{Q}Q$ pairs and then rearrange them, so as to form QQ diquark. *Then*, the QQ diquark needs to pick up a light quark q , to make a QQq baryon. At first, it seems that the production cross section for such a process is too low for the current generation of accelerators.

This view is probably overly pessimistic. A substantial basis for optimism is the observation of a large number of the doubly-heavy $B_c = (b\bar{c})$ mesons by D0, CDF and especially LHCb [28–30] indicating [11, 31] that simultaneous production of $\bar{b}b$ and $\bar{c}c$ pairs which are close to each other in space and in rapidity and can coalesce to form doubly-heavy hadrons is not too rare.

There are interesting parallels between the doubly-heavy baryons QQq and the hypothetical $QQ\bar{q}\bar{q}$ tetraquarks. In both types of systems, there is a light color triplet — a quark or an anti-diquark — bound to a heavy diquark. Because of this similarity, *experimental observation of doubly-heavy baryons is very important not just in its own right, but as a source of extremely valuable information for deducing the properties of the more exotic $QQ\bar{q}\bar{q}$ tetraquarks*. Such a deduction can be carried out just as it was done for b baryons.

In addition, doubly heavy baryons exhibit an interesting application of the heavy quark symmetry. In the limit $m_Q \rightarrow \infty$, the wave function of a light quark in a doubly heavy baryon QQq is identical to the wave function of a light quark in a heavy light meson $\bar{Q}q$. This is because in a QQq baryon, the two heavy quarks have negligible kinetic energy and in the limit $m_Q \rightarrow \infty$ they become static, sitting on top of each other and forming a color antitriplet, just like in the $\bar{Q}q$ meson. Moreover, in the $m_Q \rightarrow \infty$ limit, there are no spin-dependent interactions between the heavy and the light quarks, so it does not matter if the heavy color antitriplet is a fermion, like \bar{Q} in the $\bar{Q}q$ meson or a boson, like the QQ diquark in the QQq baryon.

Corrections to this baryon–meson relation scale like Λ_{QCD}/m_Q and are, in principle, computable. Thus, the QQq baryons will become a very useful “theoretical laboratory” for testing our ideas about bound state formation in QCD.

In the last few years, it has become possible to accurately predict at the level of 2–3 MeV the masses of heavy baryons containing the b quark: $\Sigma_b(bqq)$, $\Xi_b(bsq)$ and $\Omega_b(bss)$ [32–34], as shown in figure 7. Similar approach can be used to predict the masses of doubly-heavy baryons [31], as shown in Table IV. Using these, one can then compute the corresponding lifetimes, as shown in Table V which also shows other authors’ estimates.

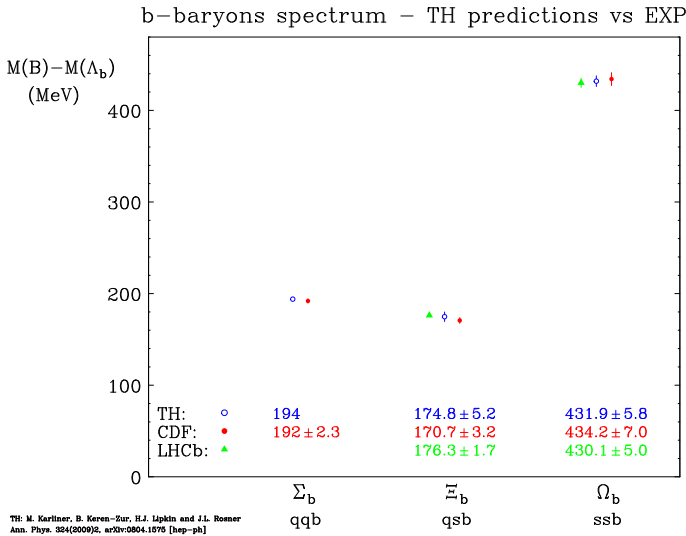


Fig. 7. Masses of b baryons — comparison of theoretical predictions [33, 34] with experiment.

TABLE IV

Summary of our mass predictions [31] (in MeV) for lowest-lying baryons with two heavy quarks. States without a star have $J = 1/2$; states with a star are their $J = 3/2$ hyperfine partners. The quark q can be either u or d . The square or curved brackets around cq denote coupling to spin 0 or 1.

State	Quark content	$M(J = 1/2)$	$M(J = 3/2)$
$\Xi_{cc}^{(*)}$	ccq	3627 ± 12	3690 ± 12
$\Xi_{bc}^{(*)}$	$b[cq]$	6914 ± 13	6969 ± 14
Ξ'_{bc}	$b(cq)$	6933 ± 12	—
$\Xi_{bb}^{(*)}$	bbq	10162 ± 12	10184 ± 12

TABLE V

Summary of lifetime predictions for baryons containing two heavy quarks. Values given are in fs.

Baryon	Our work [31]	Ref. [35]	Ref. [36]	Ref. [37]	Ref. [38]
$\Xi_{cc}^{++} = ccu$	185	430 ± 100	460 ± 50	500	~ 200
$\Xi_{cc}^+ = ccd$	53	120 ± 100	160 ± 50	150	~ 100
$\Xi_{bc}^+ = bcu$	244	330 ± 80	300 ± 30	200	—
$\Xi_{bc}^0 = bcd$	93	280 ± 70	270 ± 30	150	—
$\Xi_{bb}^0 = bbu$	370	—	790 ± 20	—	—
$\Xi_{bb}^- = bbd$	370	—	800 ± 20	—	—

The most important decay modes are those involving the most-favored Cabibbo–Kobayashi–Maskawa matrix elements, such as $c \rightarrow sW^{*+}$ and $b \rightarrow cW^{*-}$. Among the latter, we focus on those modes which can pass the trigger criteria in the collider experiments, such as:

- (a) $\Xi_{cc}^{++}(ccu) \rightarrow (csu)W^{*+} \rightarrow \Xi_c^+ \pi^+ \rightarrow \Xi^- \pi^+ \pi^+ \pi^+$, $\Lambda_c^+ K^- \pi^+ \pi^+$;
- (b) $\Xi_{cc}^+(ccd) \rightarrow (csd)W^{*+} \rightarrow \Xi_c^0 \pi^+$, $\Lambda_c^+ K^- \pi^+$;
- (c) $\Xi_{bc}^+(bcu) \rightarrow \Xi_{cc}^{++} W^{*-}$, $\Xi_b^0 W^{*+}$;
- (d) $\Xi_{bc}^0(bcd) \rightarrow \Xi_{cc}^+ W^{*-}$, $\Xi_b^- W^{*+}$, $(bsu)^*$;
- (e) $\Xi_{bb}(bbq) \rightarrow (bcq)^* W^{*-}$.

An interesting decay involving the subprocess $b \rightarrow (J/\psi s)$ twice is the chain

$$\Xi_{bb} \rightarrow J/\psi \Xi_b^{(*)} \rightarrow J/\psi J/\psi \Xi^{(*)}, \quad (3)$$

where $\Xi_b^{(*)}$ denotes a (possibly excited) state with the minimum mass of $\Xi_b(5792)$, while $\Xi^{(*)}$ denotes a (possibly excited) state with the minimum mass of Ξ . Although this mode is expected to be quite rare and one has to pay the penalty of two J/ψ leptonic branching fractions, it has a distinctive signature and is worth looking for.

In Ref. [31], we also estimated the hyperfine splitting between B_c^* and B_c mesons to be 68 MeV. P-wave excitations of the Ξ_{cc} with light-quark total angular momentum $j = 3/2$, the analog of those observed for D and B mesons, were estimated to lie around 420–470 MeV above the spin-weighted average of the Ξ_{cc} and Ξ_{cc}^* masses.

3.1. Prospects for detection

Production of baryons containing two heavy quarks requires simultaneous production of two heavy quark–antiquark pairs. Subsequently, a heavy quark from one pair needs to coalesce with a heavy quark from the other pair, forming together a color antitriplet heavy diquark. The heavy diquark then needs to pick up a light quark to finally hadronize as a doubly-heavy baryon. The coalescence of the two heavy quarks requires that they be in each other’s vicinity in both ordinary space and in rapidity space. Computation of the corresponding cross section from first principles is difficult and is subject to considerable uncertainties due to nonperturbative effects. Instead, we use existing data [28–30] and theoretical estimates [39–41] of the closely-related process of B_c production.

The two processes are closely related because production of B_c also requires simultaneous production of two heavy quark–antiquark pairs. *A priori*, B_c production has a somewhat higher probability, since in B_c production a heavy quark from one pair needs to coalesce with a heavy antiquark (rather than a quark) from the other pair and there is no need to pick up an additional light quark. There is no suppression associated with the latter, as once the color antitriplet heavy diquark is formed, it can only hadronize by picking up a light quark. On the other hand, the attraction between a quark and an antiquark is twice stronger than the attraction between two quarks and we need to estimate the corresponding suppression factor. In order to see if Ξ_{bc} and B_c production rates are comparable, it would be useful to compare the analogous production rates of Ξ_c and D_s (or Ξ_b and B_s) in experiments with large enough E_{CM} , whether in e^+e^- , $\bar{p}p$, or pp collisions.

Although it is not directly related, one may consider the relative probability of a b quark produced at high energy fragmenting into a meson (picking up a light antiquark) and a baryon (picking up a light diquark). The Heavy Flavor Averaging Group (HFAG) [42] has tabulated these quantities as measured in Z decays and the Tevatron.

According to the HFAG analysis, depending on the production mechanism, the b quark turns into a baryon between about 10 and 25% of the time. Fragmentation into a baryon is somewhat favored at low transverse momentum [42] in hadron collisions.

More recently, LHCb has carried out a thorough analysis of the b quark fragmentation into mesons and baryons [43–46]. In particular, the rather striking Fig. 4 in Ref. [46] shows that the ratio of Λ_b production to B^0 meson production for p_T below 10 GeV is above 0.3 and goes above 0.5 for lower p_T .

A crude conclusion which we might draw from this comparison is that a baryon composed of two heavy quarks could be produced with at least 10% of the B_c production rate. An even more optimistic estimate, supported by the above LHCb fragmentation data, is provided by an explicit calculation [35] which predicts the production rates for Ξ_{cc} and Ξ_{bc} to be as large as 50% of that for $(B_c + B_c^*)$ at the Tevatron, of the order of several nb. The cross section for Ξ_{bb} is estimated in that work to be about a factor of 10 less.

In [31], we computed the inclusive B_c production cross section at the LHC directly from the LHCb data, obtaining

$$\sigma(pp \rightarrow B_c + X) \approx 0.4 \mu\text{b} \quad (4)$$

for $4 < p_T < 40$ GeV and $2.5 < \eta < 4.5$. With 162 ± 18 $B_c^+ \rightarrow J/\psi\pi^+$ events, we estimated [31] an acceptance a bit below 3%. One might expect the Ξ_{cc} production cross section at LHCb to be at most a tenth of B_c cross section, *i.e.* ~ 40 nb, at 7 TeV.

There is an interesting question whether Ξ_{cc} is LHCb's best bet for discovering doubly-heavy baryons. The point is that because of Cabibbo suppression, the b quark lifetime is about 7 times longer than the c quark, even though the b quark is more than 3 times heavier and the phase space for weak quark decay of a heavy quark scales like $(m_b/m_c)^5$ times a kinematic function of the final and initial masses. Thus, $\tau(\Lambda_b) \approx 1.5 \times 10^{-12}$ s *vs.* $\tau(\Lambda_c) \approx 2 \times 10^{-13}$ s, *etc.* The difference between actual Ξ_{cc} and Ξ_{bc} lifetimes, as shown in Table III, is not so pronounced. Longer lifetime makes it much easier to identify the secondary vertex. On the other hand, the cross section for producing bottom quarks is, of course, much smaller than for charmed quarks. So there is a trade-off.

For the sake of completeness, we also provide here a brief update on the status of search for doubly charmed baryons in e^+e^- experiments. The most recent and most stringent limits in this case come from Belle [47]. They used a 980 fb^{-1} data sample to search for Ξ_{cc}^+ and Ξ_{cc}^{++} decaying into $\Lambda_c^+ K^- \pi^+(\pi^+)$ and $\Xi_c^0 \pi^+(\pi^+)$ final states.

Theoretical predictions for the inclusive cross section $\sigma(e^+e^- \rightarrow \Xi_{cc} + X)$ at Belle CM energy, $\sqrt{s} = 10.58 \text{ GeV}$, vary over a rather wide range, from 70 fb [48] to 230 fb [49].

The CM energy of the B factories is sufficient only for production of Ξ_{cc} , as Ξ_{bc} and Ξ_{bb} are too heavy. So, within the foreseeable future, the latter can only be produced at LHC and perhaps at RHIC.

As in the case of doubly-heavy baryon production in LHCb, there is a significant uncertainty in theoretical predictions for the inclusive cross section $\sigma(e^+e^- \rightarrow \Xi_{cc} + X)$. Therefore, we suggest another approach, similar in spirit to what we proposed for LHCb. This approach is again directly based on observables which are, in principle, accessible in e^+e^- machines.

One can make a rough estimate of the doubly-charmed baryon production rate by assuming that the suppression of ccq baryons Ξ_{cc} vs. csq baryons Ξ_c is of the same order of magnitude as the suppression of Ξ_c vs. ssq baryons Ξ [31]. The physical content of this assumption is that the suppression due to replacing an s quark in a baryon by a much heavier c quark is approximately independent of the spectator quarks in the baryon

$$\sigma(e^+e^- \rightarrow \Xi_{cc} + X) \sim \sigma(e^+e^- \rightarrow \Xi_c + X) \frac{\sigma(e^+e^- \rightarrow \Xi_c + X)}{\sigma(e^+e^- \rightarrow \Xi + X)}. \quad (5)$$

The approximate formula in Eq. (5) and its generalizations to Ξ_{bc} and Ξ_{bb} production should also apply to pp collisions:

$$\begin{aligned} \sigma(pp \rightarrow \Xi_{bc} + X) &\sim \sigma(pp \rightarrow \Xi_b + X) \frac{\sigma(pp \rightarrow \Xi_c + X)}{\sigma(pp \rightarrow \Xi + X)} \\ &\sim \sigma(pp \rightarrow \Xi_c + X) \frac{\sigma(pp \rightarrow \Xi_b + X)}{\sigma(pp \rightarrow \Xi + X)} \end{aligned} \quad (6)$$

as well as

$$\sigma(pp \rightarrow \Xi_{bb} + X) \sim \sigma(pp \rightarrow \Xi_b + X) \frac{\sigma(pp \rightarrow \Xi_b + X)}{\sigma(pp \rightarrow \Xi + X)}. \quad (7)$$

We are optimistic that with the increased data samples soon to be available in hadronic and e^+e^- collisions, the first baryons with two heavy quarks will finally be seen.

4. The new spectroscopy in future high- E high- \mathcal{L} e^+e^- colliders

Several high-energy high-luminosity future e^+e^- colliders are currently under discussion. Their primary task is to look for physics beyond the Standard Model. Yet, through initial state radiation, it might be possible to use them to explore interesting physics *significantly below* their design E_{CM} . Such machines may turn out to be our best chance at exploring the rich new QCD spectroscopy of doubly-heavy hadrons [50].

The basic idea is very simple: An electron–positron collider operating at a center-of-mass energy E_{CM} can collect events at all lower energies through initial-state radiation (ISR), as schematically indicated in Fig. 8.

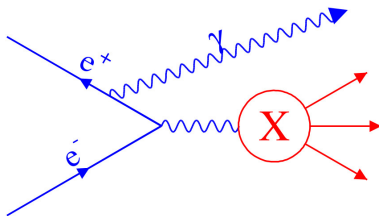


Fig. 8. Schematic depiction of the radiative return process in an e^+e^- collider. Before the collision, one of the leptons emits a hard photon, thereby significantly reducing the center-of-mass energy of available for e^+e^- annihilation into the final state X .

From the point of view of the accelerator designers such events at lower energies are usually viewed as a nuisance. But from our point of view, they are an opportunity — *it's not a bug, it's a feature!*

This *radiative return* process has been used to good advantage in e^+e^- colliders such as DAΦNE, PEP-II, KEK-B, and LEP [51–54].

In a recent paper [50], we explored the capabilities of a higher-energy high-luminosity e^+e^- collider such as that envisioned by CERN (FCC-ee) [55] or China (CEPC) [56], operating at $E_{\text{CM}} \simeq 250$ or 90 GeV (functioning as a Giga- or Tera- Z factory at the latter energy) [57], to perform radiative return studies of physics at lower center-of-mass energies. Our result provides a preliminary indication that such machines can fill in the gaps left by PEP, PETRA, TRISTAN and LEP, shown in Fig. 9.

The most interesting potential applications include dark photon searches and heavy quark exotic spectroscopy.

As the first step, in order to fairly assess the capabilities of future colliders with past and present colliders, it is necessary to specify the total integrated luminosity expected to be collected by future colliders.

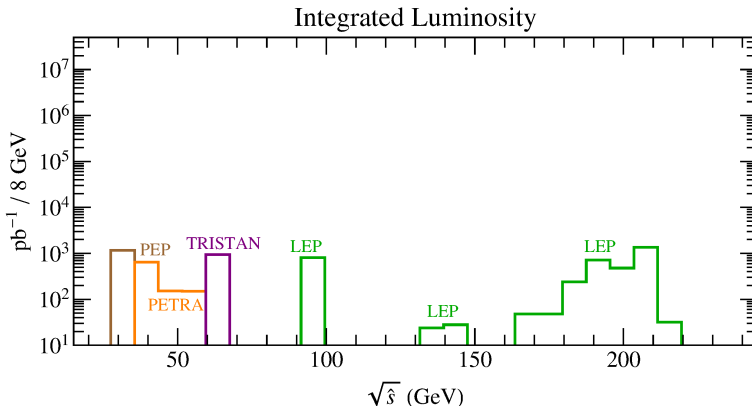


Fig. 9. Gaps in e^+e^- integrated luminosity coverage left by PEP, PETRA, TRISTAN and LEP at center-of-mass energies above B factories.

Based on current design reports, over 2 interaction points the CEPC is expected to collect 500 fb^{-1} on the Z pole, which corresponds to approximately 1×10^{10} Z s, and 5 ab^{-1} at $E_{\text{CM}} \simeq 250 \text{ GeV}$ [58]. The FCC-ee, over 4 interaction points, is expected to collect 50 ab^{-1} , which is roughly 1×10^{12} Z s, at $E_{\text{CM}} \simeq 90 \text{ GeV}$ and 10 ab^{-1} at $E_{\text{CM}} \simeq 250 \text{ GeV}$ [59]. Table VI summarizes these numbers. For convenience, where the exact number of events is not important, we shall occasionally quote results for a nominal integrated luminosity of 1 ab^{-1} . These values may be rescaled appropriately.

TABLE VI

Projected luminosities for the CEPC [58] and FCC-ee [59]. These values are used throughout the text.

	$\sqrt{s} = 90 \text{ GeV}$	$\sqrt{s} = 250 \text{ GeV}$
CEPC	0.5 ab^{-1}	5 ab^{-1}
FCC-ee	50 ab^{-1}	10 ab^{-1}

5. Some previous uses of radiative return

Considerable use has been made of radiative return in previous experiments using electron–positron colliders. In Table VII, we summarize some parameters of experiments at these colliders [60, 61]. Maximum instantaneous luminosities of circular e^+e^- colliders are plotted *versus* year in Fig. 10.

TABLE VII

Instantaneous and/or integrated luminosities achieved at some e^+e^- colliders. Based in part on Section 30 of Ref. [60], with values from Ref. [61] for PETRA, PEP, and TRISTAN. We thank G. Alexander and S.L. Wu for help with some of these estimates.

Collider	Detector	CM energy [GeV]	Max. \mathcal{L} [$10^{30} \text{ cm}^{-2}\text{s}^{-1}$]	$\int \mathcal{L} dt$ [fb $^{-1}$]
DAΦNE	KLOE	1.02	453	2.5
		1.00	453	0.23
CESR	CLEO	9.46–11.30	1280 at 10.6 GeV	15.1
PEP-II	BaBar	10.58	12069	424.7
		10.18	...	43.9
KEK-B	Belle	9.46–10.89	21083	980
PEP		29	60	1.167 ^a
PETRA		46.8 ^b	24 at 35 GeV	0.817 ^c
TRISTAN		64 ^b	40	0.942 ^d
LEP		M_Z	24	0.808 ^e
		> 130	34–90	2.980 ^e

^aSummed over detectors DELCO, HRS, MAC, Mark II, TPC/2 γ .

^bMaximum value.

^cSummed over detectors CELLO, JADE, Mark J, PLUTO, TASSO.

^dSummed over detectors AMY, TOPAZ, VENUS.

^eSummed over detectors ALEPH, DELPHI, L3, OPAL.

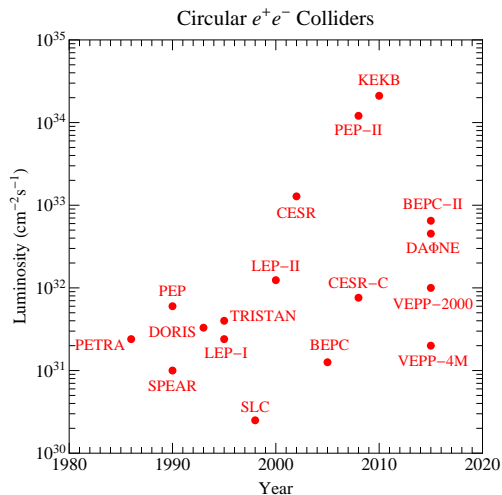


Fig. 10. Maximum instantaneous luminosities of circular e^+e^- colliders *versus* time. Adapted from Fig. 1 of Ref. [62].

6. Radiative return in narrow resonance production

As the first example, let us discuss how radiative return works in the case of a narrow resonance.

The cross section for electron–positron production of a vector meson resonance R with mass m_R and e^+e^- partial width Γ_{ee} decaying to a final state f with partial width Γ_f may be written near resonance as

$$\sigma(e^+e^- \rightarrow R \rightarrow f; s) = \frac{12\pi\Gamma_{ee}\Gamma_f}{(s - m_R^2)^2 + (m_R\Gamma_R)^2}, \quad (8)$$

where $s = E_{\text{CM}}^2$, and m_R and Γ_R are the resonance mass and total width.

For the $\Upsilon(4S)$, whose decays are almost exclusively to $B\bar{B}$ final states, the leptonic branching ratio is quoted by the Particle Data Group [60] as 1.57×10^{-5} , while the total width is 20.5 MeV, leading to a leptonic partial width $\Gamma_{ee} = 0.322$ keV. We shall use this value, noting that it is mildly inconsistent with the Particle Data Group's average of 0.272 keV. The mass is 10.5794 ± 0.0012 GeV; the cross section at the resonance peak is about 2.06 nb. The resonance shape is shown at the left in Fig. 11.

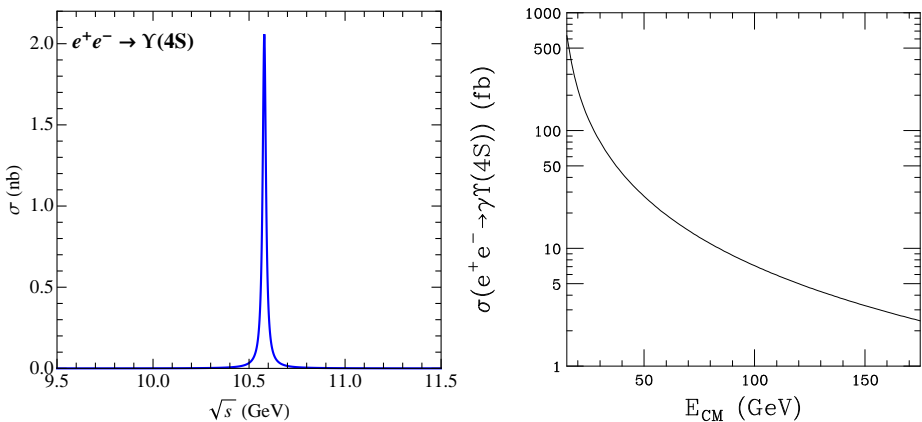


Fig. 11. Cross section for $e^+e^- \rightarrow \Upsilon(4S)$ (left) and including the emission of a photon at an e^+e^- collider with CM energy E_{CM} (right).

A resonance R may be produced by the radiative return process $e^+e^- \rightarrow \gamma R$, where the electron or positron of beam energy $E = E_{\text{CM}}/2$ radiates a fraction $1 - x$ of its energy and is left with energy xE . Neglecting the small electron mass, the squared effective mass of the e^+e^- system is then xs . An electron beam of energy E radiates a photon and ends up with an energy xE with a probability per unit x [63] denoted by

$$f_e(x, \sqrt{s}, p_{\text{T,cut}}) = \frac{\alpha}{\pi} \frac{1+x^2}{1-x} \ln \frac{E}{p_{\text{T,cut}}}, \quad (9)$$

where the minimum photon transverse momentum $p_{T,\text{cut}}$ provides a collinear cutoff². In the absence of an explicit choice of cutoff, it is provided by the electron mass m_e , which we shall use in much of what follows. The cross section for production of the resonance R by radiative return, where R decays to the final state f , is then

$$\sigma(e^+e^- \rightarrow \gamma R \rightarrow \gamma f) = \frac{2\alpha}{\pi} \ln \frac{E}{m_e} \int_0^1 dx \frac{1+x^2}{1-x} \sigma(e^+e^- \rightarrow R \rightarrow f; xs), \quad (10)$$

where the factor of two comes from the fact that either lepton can radiate the photon. In the narrow-resonance approximation, the integral in this expression can be done in closed form, with the result

$$\sigma(e^+e^- \rightarrow \gamma R \rightarrow \gamma f) \simeq 24\alpha\pi \ln \frac{E}{m_e} \frac{1+x_0^2}{1-x_0} \frac{\Gamma_{ee}\mathcal{B}_f}{m_R s}, \quad (11)$$

where $x_0 = m_R^2/s$ and $\mathcal{B}_f = \Gamma_f/\Gamma_R$ denotes the branching fraction into the final state f . The cross section for $e^+e^- \rightarrow \Upsilon(4S)$ including the emission of a photon is shown as a function of e^+e^- CM energy in Fig. 11 (right).

The proposed high-energy electron–positron colliders at CERN and in China anticipate integrated luminosities of 50 ab^{-1} and 0.5 ab^{-1} , respectively, at CM energy of 90 GeV, and 10 ab^{-1} and 5 ab^{-1} , respectively, at 250 GeV [58, 59]. The observation of a new resonance with at least 10 events would then require cross sections of at least 0.2 and 20 ab at CERN or China, respectively, at 90 GeV, or at least 1 and 2 ab, respectively, at 250 GeV.

Figure 12 illustrates contours of equal cross section for an e^+e^- collider with CM energy 90 (left) and 250 (right) GeV to produce a resonance of mass m_R via radiative return. These results imply a cross section of 9.17 fb for the $\Upsilon(4S)$ produced by radiative return at $E_{\text{CM}} = 90$ GeV, given an assumed leptonic partial width of $\Gamma_{ee} = 0.322 \text{ keV}$ [60]. For a given E_{CM} , the lowest sensitivity appears to occur for a resonance mass roughly equal to $E_{\text{CM}}/2$, *i.e.*, the beam energy.

The results of Fig. 12 can be expressed in more universal form. In the narrow-resonance approximation, the predicted radiative return cross section, Eq. (11), is directly proportional to $\Gamma_{ee}\mathcal{B}_f$, so the ratio $\sigma(e^+e^- \rightarrow \gamma R \rightarrow \gamma f)/\Gamma_{ee}\mathcal{B}_f$ is a function only of s and m_R . In Fig. 13, we plot this ratio as a function of resonance mass for two values of E_{CM} .

² The numerator of the logarithm is sometimes taken to be $2E = \sqrt{s}$.

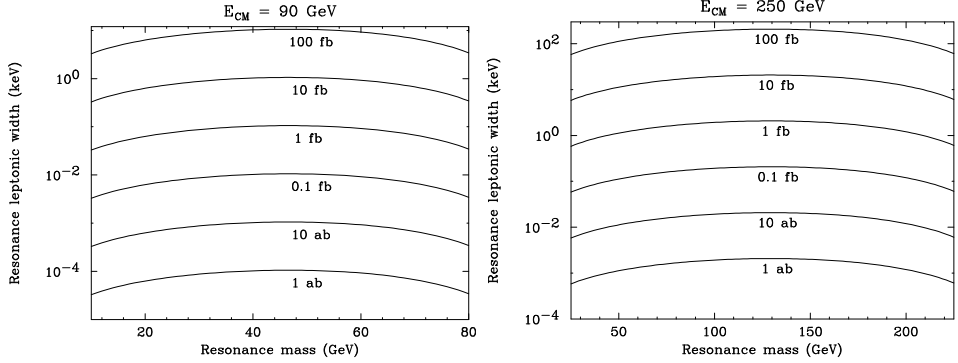


Fig. 12. Contours of equal cross section for radiative return production of a resonance with leptonic width Γ_{ee} (assuming 100% branching fraction to a final state f). Left: $E_{\text{CM}} = 90$ GeV; right: $E_{\text{CM}} = 250$ GeV.

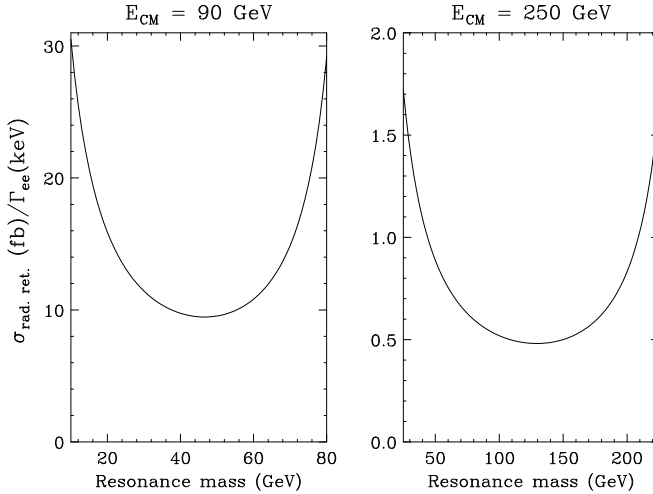


Fig. 13. $\sigma(e^+e^- \rightarrow \gamma R \rightarrow \gamma f)/\Gamma_{ee}\mathcal{B}_f$ as a function of resonance mass for $E_{\text{CM}} = 90$ (left) and 250 (right) GeV.

7. Continuum production

An important quantity is the effective luminosity of a high-energy collider for studying any given process at lower center-of-mass energy. Defining $\sigma(s) \equiv \sigma(e^+e^- \rightarrow \gamma f; s)$ and $\hat{\sigma}(\hat{s}) \equiv \sigma(e^+e^- \rightarrow f; \hat{s})$ for a given final state f , the relation between the two is

$$\frac{d\sigma(s)}{dx} = \frac{2\alpha}{\pi} \frac{1+x^2}{1-x} \ln \frac{E}{m_e} \hat{\sigma}(\hat{s}), \quad (12)$$

where $x = \hat{s}/s$. The subsystem CM energy may be denoted $\hat{E}_{\text{CM}} = \sqrt{\hat{s}}$. The cross section per unit \hat{E}_{CM} times an interval Δ of \hat{E}_{CM} is then

$$\begin{aligned} \frac{d\sigma(s)}{d\hat{E}_{\text{CM}}} \Delta &= \frac{4\alpha\hat{E}_{\text{CM}}}{\pi s} \frac{1+x^2}{1-x} \Delta \ln \frac{E}{m_e} \hat{\sigma}(\hat{s}) \\ &\equiv L_f \hat{\sigma}(\hat{s}), \end{aligned} \quad (13)$$

where L_f is the *fractional luminosity* per \hat{E}_{CM} bin of size Δ . Examples of this function for a bin width of $\Delta = 1$ GeV are shown in the top curves of Fig. 14.

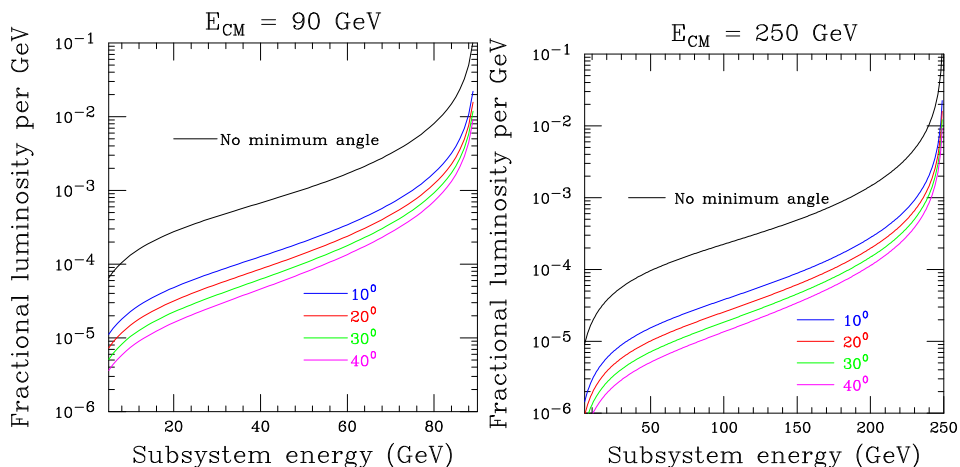


Fig. 14. Fractional luminosity L_f as a function of subsystem energy \hat{E}_{CM} for $E_{\text{CM}} = 90$ (left) and 250 (right) GeV. Top curves: No minimum angle; infrared cutoff provided by $\ln(E/m_e)$ [Eq. (13)]. Lower curves, top to bottom: $\theta_0 = 10, 20, 30, 40^\circ$.

For low \hat{E}_{CM} , one may take $(1+x^2)/(1-x) \simeq 1$ in Eq. (13). Integrating from $\hat{E}_{\text{CM}}^{\text{min}} = 10$ GeV to $\hat{E}_{\text{CM}}^{\text{max}} = 30$ GeV, one then finds

$$L_f = \frac{2\alpha}{\pi s} \left[\left(\hat{E}_{\text{CM}}^{\text{max}} \right)^2 - \left(\hat{E}_{\text{CM}}^{\text{min}} \right)^2 \right] \ln \frac{E}{m_e}. \quad (14)$$

For $E_{\text{CM}} = (90, 250)$ GeV, we find $L_f = (5.22, 0.74) \times 10^{-3}$. For a total of 1 ab^{-1} at $E_{\text{CM}} = (90, 250)$ GeV, this then provides a total integrated luminosity of $(5220, 740) \text{ pb}^{-1}$ in the range of $10 \leq \hat{E}_{\text{CM}} \leq 30$ GeV. This exceeds integrated luminosities at PEP or PETRA (see Table VII).

Given the concept of fractional luminosity, we can compute the effective luminosity gathered at each center-of-mass energy via radiative return. This effective luminosity can then be plotted together with the integrated luminosity of earlier accelerators, shown in Fig. 9. The result is shown in Fig. 15 for $\sqrt{s} = 90$ and 250 GeV compared to the luminosity collected directly at various other colliders. This figure clearly shows that a high-luminosity high-energy e^+e^- collider both competes with and fills in gaps left by previous colliders.

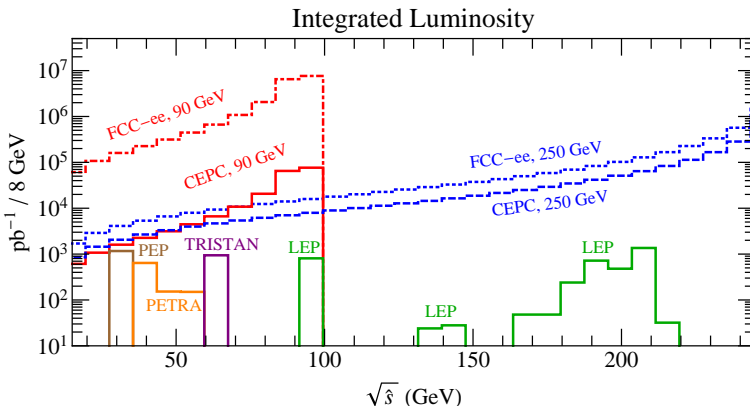


Fig. 15. Integrated luminosity from past low energy e^+e^- colliders at their nominal center-of-mass energies compared to the effective luminosity through radiative return from future e^+e^- colliders at $\sqrt{s} = 90$ or 250 GeV (no minimum angle; see Fig. 14 for effects of minimum angles). The FCC-ee curves assume an integrated luminosity of 50 ab^{-1} at 90 GeV and 10 ab^{-1} at 250 GeV. The CEPC curves assume an integrated luminosity of 0.5 ab^{-1} at 90 GeV and 5 ab^{-1} at 250 GeV. Integrated luminosities of PEP-II and Belle (Table VII) exceed those achievable by radiative return at FCC-ee or CEPC running at 90 or 250 GeV.

Cleaner signals for radiative return may be obtained at the expense of number of recorded events by demanding that the radiated photon make a minimum angle θ_0 with respect to the beam axis. Let θ be the polar angle of the radiated photon, and $z \equiv \cos \theta$, $z_0 \equiv \cos \theta_0$. Using Eq. (8) of [64], we find that the angular distribution of the radiated photon for $m_e = 0$ is given by

$$\frac{d^2\sigma(s)}{d\hat{E}_{\text{CM}}dz} = \frac{4\alpha\hat{E}_{\text{CM}}}{\pi s} \frac{\hat{\sigma}(\hat{s})}{1-z^2} \left[\frac{1-x}{4} (1+z^2) + \frac{x}{1-x} \right]. \quad (15)$$

This may be integrated between the desired limits of θ , with the result

$$\int_{-z_0}^{z_0} dz \frac{d^2\sigma(s)}{d\hat{E}_{\text{CM}} dz} = \frac{4\alpha\hat{E}_{\text{CM}}}{\pi s} \hat{\sigma}(\hat{s}) \left[\frac{1-x}{2} \left(\ln \frac{1+z_0}{1-z_0} - z_0 \right) + \frac{x}{1-x} \ln \frac{1+z_0}{1-z_0} \right]. \quad (16)$$

The ratio between the left-hand side and $\hat{\sigma}(\hat{s})$ is again a fractional luminosity and is shown by the lower curves in Fig. 14, again for a bin width of 1 GeV. In the limit of small $\theta_0 \simeq p_{\text{T}}/E_{\gamma}$, the leading-logarithmic term of Eq. (16) reduces to the form in Eq. (13).

8. Potential applications

8.1. Dark photon search

We focus here on the 10s to 100s of GeV scale. For simplicity, we assume that a “dark photon”, denoted by Z' , is kinetically mixed with a hypercharge gauge boson with amplitude ϵ

$$\mathcal{L} = -\frac{1}{4}\hat{B}_{\mu\nu}^2 - \frac{1}{4}\hat{Z}'_{\mu\nu}{}^2 + \epsilon \frac{1}{2c_w} \hat{Z}'_{\mu\nu} \hat{B}^{\mu\nu} + \frac{1}{2}M_{Z'}^2 \hat{Z}'_{\mu}{}^2, \quad (17)$$

where c_w is the cosine of the Weinberg angle and the hats denote states that are not mass eigenstates. After diagonalization, one finds a single massless state identified to be the photon. The would-be standard model Z and dark photon Z' also mix due to electroweak symmetry breaking.

The dark photon inherits couplings to fermions both from mixing with hypercharge and mixing with the Z . In the limit $\epsilon \ll 1$ and $M_{Z'} \ll M_Z$, the dark photon couplings to fermions become photon-like and the partial width simplifies to

$$\Gamma(Z' \rightarrow f\bar{f}) = \frac{\alpha M_{Z'}}{3} Q_f^2 N_c \beta_f \left(\frac{3 - \beta_f^2}{2} \right) \epsilon^2, \quad (18)$$

where there are N_c colors of f with charge Q_f and mass m_f , and

$$\beta_f^2 \equiv 1 - \frac{4m_f^2}{M_{Z'}^2}. \quad (19)$$

Ignoring all quark masses except m_b and assuming the top–antitop channel is closed, the branching ratio of Z' into $\mu^+\mu^-$ (a convenient and low-background final state) is

$$\mathcal{B}(Z' \rightarrow \mu^+\mu^-) = 3 \left(19 + \frac{\beta_b(3 - \beta_b^2)}{2} \right)^{-1}. \quad (20)$$

When $M_{Z'} \approx M_Z$, the dark photon couplings become Z -like and when $M_{Z'} \gg M_Z$, they become B -like. This can be seen in Fig. 16, where we show the branching ratios, assuming the dark photon decays entirely into Standard Model particles. These are computed using $\epsilon = 5 \times 10^{-3}$ although for $\epsilon \ll 1$, the branching ratios are independent of ϵ . For simplicity, we only use the perturbative calculation. For low Z' masses, *i.e.*, below a few GeV, it is necessary to consider threshold effects, QCD corrections, and hadronic resonances.

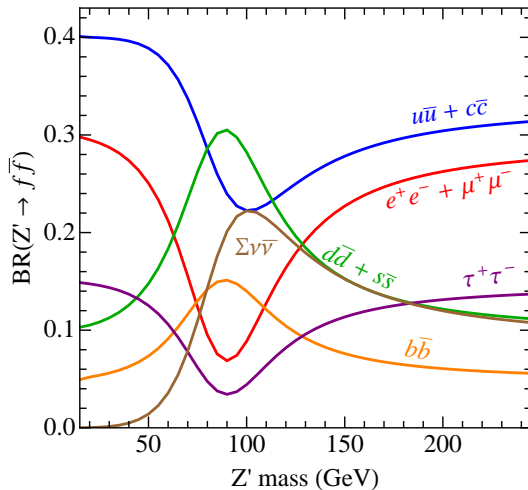


Fig. 16. Dark photon branching ratios. These are computed using $\epsilon = 5 \times 10^{-3}$ although for $\epsilon \ll 1$ the branching ratios are independent of ϵ .

The results for the reach of an e^+e^- collider in search for a dark photon are shown in Fig. 17. The current and projected limits from electroweak precision data (EWPT) were computed in [65].

8.2. Leptonic production of $b\bar{b}$

The asymmetric B factories PEP-II and KEK-B have explored $b\bar{b}$ production up to CM energies of about 11 GeV with compelling statistics, and the upgraded KEK-B with the Belle-II detector will extend samples to dozens of events per attobarn. However, from about 11 to 90 GeV, the e^+e^- territory is much more sparsely populated with data, as one can see from Table VII and Fig. 15. Radiative return studies from a Giga- Z or Tera- Z factory can help to fill this gap. A sample process is $e^+e^- \rightarrow (\gamma^*, Z^*) \rightarrow b\bar{b}$, compared for direct production with the radiative return process $e^+e^- \rightarrow (\gamma^*, Z^*) \gamma_{\text{ISR}} \rightarrow b\bar{b} \gamma_{\text{ISR}}$. The results are compared with the direct process in Table VIII.

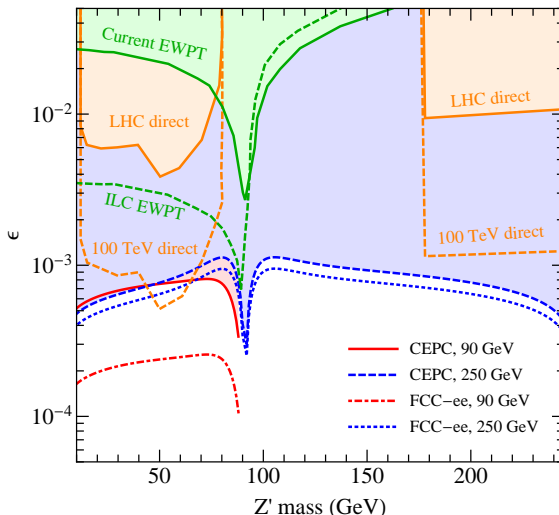


Fig. 17. Dark photon limits at 95% C.L. on the hypercharge mixing ϵ as a function of dark photon mass. The $\sqrt{s} = 90$ GeV and 250 GeV lines show our projections with future e^+e^- colliders with integrated luminosities specified in Table VI. Electroweak precision constraints (EWPT) and direct searches are taken from [65]. The 100 TeV projection assumes an integrated luminosity of 3000 fb^{-1} .

TABLE VIII

 Comparison of direct and radiative-return e^+e^- production of $b\bar{b}$.

Collider	Direct			\hat{E} range [GeV]	Radiative return			
	σ [pb]	$\int \mathcal{L} dt$ [pb^{-1}]	Events (10^3)		$\sqrt{s} = 90$ GeV σ [pb]	$\sqrt{s} = 90$ GeV Evs. (10^6) ^a	$\sqrt{s} = 250$ GeV σ [pb]	$\sqrt{s} = 250$ GeV Evs. (10^3) ^b
PEP	36.8	1167	42.9	10–35	0.494	(24.5,0.245)	0.066	(660,330)
PETRA	25.8	817	21.1	35–60	0.410	(20.5,0.205)	0.039	(391,196)
TRISTAN	16.2	942	15.3	60–85	12.94	(647,6.47)	0.256	(2562,1281)

^aAssuming $\int \mathcal{L} dt = (50, 0.5) \text{ ab}^{-1}$ at (FCC-ee, CEPC).

^bAssuming $\int \mathcal{L} dt = (10, 5) \text{ ab}^{-1}$ at (FCC-ee, CEPC).

8.3. Heavy flavor spectroscopy

There are many possible applications of radiative return to heavy flavor spectroscopy.

- (a) Bottomonium analogues of charmonium X, Y, Z states

By now, there is a lot of data on the X, Y, Z states. These states contain a $c\bar{c}$ pair, but their properties do not agree with those expected from excited charmonia. Some of them are manifestly exotic and must

contain an additional $\bar{q}q$ pair of light quarks. Also for those which are not manifestly exotic, there is substantial indirect evidence of an additional $\bar{q}q$ pair. In any case, the details of the internal structure of these states are not known, in the sense that we do know for sure the dominant spatial configurations of the quarks from which they are built.

We do know, however, that the various charmed X , Y , Z states are almost certain to have their counterparts in the bottomonium sector. Studying these analogues will provide valuable information which will be crucial for testing the various theoretical models.

- (b) Bottom analogues of $D_{s0}^*(2317)$ and $D_{s1}(2460)$:

The process $e^+e^- \rightarrow B_{sJ} + X$ may be used to look for B_{sJ} states, b -quark analogues of the very narrow D_{sJ} states seen by BaBar, CLEO and Belle [66–68]: $D_{s0}(2317)$ with $J^P = 0^+$ and $m[D_{s1}(2460)]$ with $J^P = 1^+$. These states have been conjectured to be the chiral partners of D_s , $J^P = 0^-$ and D_s^* , $J^P = 1^-$, respectively [69, 70]. A strong hint toward this conjecture is supplied by the almost equal splitting between the states of opposite parity [60]: $m[D_{s0}(2317)] - m[D_s] = 349.4 \pm 0.6$ MeV $\approx m[D_{s1}(2460)] - m[D_s^*] = 347.3 \pm 0.7$ MeV \approx constituent mass of light quarks.

There are detailed and highly interesting predictions for the bottom analogues of these states. Observing them experimentally will provide a golden opportunity to test our understanding of chiral symmetry breaking (χ SB). The relevant thresholds are discussed in item (d) below.

- (c) Doubly-heavy exotic hadrons, incl. bottom-charm exotics: \bar{B}^*D^* , *etc.*

In the first part of this paper, we discussed exotic hadrons which lie close to the $\bar{D}D^*$, \bar{D}^*D^* , $\bar{B}B^*$ and \bar{B}^*B^* thresholds. As we have seen, in addition to these states which contain hidden charm or bottom quantum numbers, there are good reasons to expect exotics with open charm and bottom, near \bar{B}^*D^* thresholds, *etc.*

- (d) Interesting thresholds

In Table IX, we summarize some thresholds for heavy flavor production in e^+e^- collisions.

Here, we have used masses tabulated in Ref. [60]. The state B_{s0} in Table IX is the expected analogue, with $J^P = 0^+$, of the $D_{s0}(2317)$, which is narrow because it lies below DK threshold. In order to produce the B_{s0} in e^+e^- collisions, it must be accompanied by a \bar{B}_s^* or

heavier companion. Angular momentum and parity conservation forbid the process $e^+e^- \rightarrow \gamma^* \rightarrow B_{s0}\bar{B}_s$. The B_{s0} mass is estimated to be 5717 MeV by assuming that D_{s0} and D_{s0} are chiral partners of D_s and B_s and, therefore, the B_{s0} - B_s splitting is very close to the D_{s0} - D_s splitting [69, 70]. On the other hand, in order for B_{s0} to be interesting, it needs to be narrow. In analogy with D_{s0} which is narrow because it is below the DK threshold, B_{s0} needs to be below BK threshold, *i.e.*, below 5778 MeV. So, in any case, the interesting threshold is between $5717 \text{ MeV} + m_{B_s^*}$ and $5778 \text{ MeV} + m_{B_s^*}$, *i.e.*, between 11132 MeV and 11193 MeV.

TABLE IX

Some thresholds for heavy flavor production in e^+e^- collisions.

Final state	Threshold [MeV]
$B\bar{B}$	10559
$B\bar{B}^*$	10605
$B^*\bar{B}^*$	10650
$B_s\bar{B}_s$	10734
$B_s\bar{B}_s^*$	10782
$B_s^*\bar{B}_s^*$	10831
$B_{s0}\bar{B}_s^*$	11132–11193 ^a
$\Lambda_b\bar{\Lambda}_b$	11239
$B_c\bar{B}_c$	12551
$B_c\bar{B}_c^*$	12619–12635 ^b
$B_c^*\bar{B}_c^*$	12687–12719 ^b
$\Xi_{bc}\bar{\Xi}_{bc}$	13842–13890 ^c
$\Xi_{bb}\bar{\Xi}_{bb}$	20300–20348 ^c

^aSee the text.

^bWith estimated B_c^* - B_c splitting 68–84 MeV [31].

^cEstimate in [31].

(e) Doubly-heavy QQq baryons

The doubly-heavy baryons were discussed in Sec. 3. Here, I want to reiterate that experimental observation of doubly-heavy baryons is very important not just in its own right, but as a source of extremely valuable information about QCD in the nonperturbative regime. Since the two heavy quarks carry very little kinetic energy, doubly-heavy baryons effectively contain only one dynamical quark. Therefore, from theoretical point of view, they are the simplest baryons and can serve as a sort of “hydrogen atom” of baryonic physics, where the calculations are relatively straightforward and can be tested against experiment.

9. Summary

A simple and consistent picture emerges from Belle, BaBar, BES, CLEO and LHCb data: the new narrow exotic mesons are loosely bound $J^P = 1^+$ states of $\bar{D}D^*$, \bar{D}^*D^* , $\bar{B}B^*$ and \bar{B}^*B^* .

This picture has led to several predictions, some of which have already been confirmed experimentally: \bar{D}^*D^* in $I = 0$ and $I = 1$ channels, new isosinglet $\bar{B}B^*$ and \bar{B}^*B^* states X_b and X_b^* below the respective two meson thresholds, and a narrow D^*B^* resonance. It has also been pointed out that the state reported and identified by ATLAS, D0 and LHCb as excited bottomonium resonance $\chi_{1b}(3P)$ might, in fact, be a mixture of X_b and $\chi_{1b}(3P)$, in analogy with $X(3872)$, which is likely a mixture of a $\bar{D}D^*$ hadronic molecule and $\chi_{1c}(2P)$ excited charmonium.

In addition to resonances near thresholds of two heavy mesons, we expect resonances near thresholds of a heavy baryon and a heavy meson or of two heavy baryons. The lightest of these resonances has already been observed by LHCb, about 10 MeV below $\Sigma_c D^*$ threshold. Other states include resonances near the thresholds of $\Sigma_b B^*$, $\Sigma_b D^*$, $\Sigma_Q \bar{\Lambda}_{Q'}$, $\Sigma_Q^+ \Sigma_Q^-$, etc.

Beyond the doubly-heavy exotic hadrons, we also expect an experimental observation of nonexotic doubly-heavy baryons in e^+e^- and hadron machines. Their discovery will be very valuable for deeper understanding of QCD in nonperturbative regime. We are sure the doubly-heavy baryons exist, so the main issue is attaining a sufficient event rate and focusing on suitable detection channels.

A future generation of high-energy high-luminosity e^+e^- colliders, utilized in radiative return mode, might provide a powerful tool for copious production of these new hadrons.

These lectures are based on recent joint work with Jon Rosner, Matthew Low, Lian-Tao Wang and Shmuel Nussinov. The new results reported here owe a great deal to an earlier long-term collaboration with the late Harry Lipkin.

REFERENCES

- [1] K.F. Chen *et al.* [Belle Collaboration], *Phys. Rev. Lett.* **100**, 112001 (2008) [[arXiv:0710.2577](#) [hep-ex]].
- [2] M. Karliner, H.J. Lipkin, [arXiv:0802.0649](#) [hep-ph].
- [3] I. Adachi *et al.* [Belle Collaboration], [arXiv:1105.4583](#) [hep-ex].
- [4] A. Bondar *et al.* [Belle Collaboration], *Phys. Rev. Lett.* **108**, 122001 (2012) [[arXiv:1110.2251](#) [hep-ex]].

- [5] M.B. Voloshin, L.B. Okun, *JETP Lett.* **23**, 333 (1976) [*Pisma Zh. Eksp. Teor. Fiz.* **23**, 369 (1976)].
- [6] N.A. Törnqvist, *Phys. Rev. Lett.* **67**, 556 (1991); *Z. Phys. C* **61**, 525 (1994) [arXiv:hep-ph/9310247].
- [7] N.A. Törnqvist, *Phys. Lett. B* **590**, 209 (2004) [arXiv:hep-ph/0402237].
- [8] M. Ablikim *et al.* [BESIII Collaboration], arXiv:1303.5949 [hep-ex].
- [9] M. Karliner, H.J. Lipkin, N.A. Törnqvist, arXiv:1109.3472 [hep-ph].
- [10] M. Karliner, H.J. Lipkin, N.A. Törnqvist, *Nucl. Phys. Proc. Suppl.* **225–227**, 102 (2012).
- [11] M. Karliner, S. Nussinov, *J. High Energy Phys.* **1307**, 153 (2013) [arXiv:1304.0345 [hep-ph]].
- [12] M. Ablikim *et al.* [BESIII Collaboration], *Phys. Rev. Lett.* **112**, 132001 (2014) [arXiv:1308.2760 [hep-ex]].
- [13] M. Ablikim *et al.* [BESIII Collaboration], *Phys. Rev. Lett.* **111**, 242001 (2013) [arXiv:1309.1896 [hep-ex]].
- [14] I thank Roman Mizuk for discussion on this point.
- [15] S. Chatrchyan *et al.* [CMS Collaboration], arXiv:1309.0250 [hep-ex].
- [16] G. Aad *et al.* [ATLAS Collaboration], *Phys. Rev. Lett.* **108**, 152001 (2012).
- [17] V.M. Abazov *et al.* [D0 Collaboration], *Phys. Rev. D* **86**, 031103 (2012) [arXiv:1203.6034 [hep-ex]].
- [18] R. Aaij *et al.* [LHCb Collaboration], *Eur. Phys. J. C* **74**, 3092 (2014) [arXiv:1407.7734 [hep-ex]].
- [19] R. Aaij *et al.* [LHCb Collaboration], *J. High Energy Phys.* **1410**, 088 (2014) [arXiv:1409.1408 [hep-ex]].
- [20] M. Karliner, J.L. Rosner, *Phys. Rev. D* **91**, 014014 (2015) [arXiv:1410.7729 [hep-ph]].
- [21] M. Karliner, J.L. Rosner, *Phys. Rev. Lett.* **115**, 122001 (2015) [arXiv:1506.06386 [hep-ph]].
- [22] R. Aaij *et al.* [LHCb Collaboration], *Phys. Rev. Lett.* **115**, 072001 (2015) [arXiv:1507.03414 [hep-ex]].
- [23] M. Karliner, H.J. Lipkin, N.A. Törnqvist, unpublished and arXiv:1109.3472 [hep-ph].
- [24] J.P. Ader, J.M. Richard, P. Taxil, *Phys. Rev. D* **25**, 2370 (1982).
- [25] A.V. Manohar, M.B. Wise, *Nucl. Phys. B* **399**, 17 (1993) [arXiv:hep-ph/9212236].
- [26] B.A. Gelman, S. Nussinov, *Phys. Lett. B* **551**, 296 (2003) [arXiv:hep-ph/0209095].
- [27] Y. Frishman, M. Karliner, *J. High Energy Phys.* **1308**, 096 (2013) [arXiv:1305.6457 [hep-ph]].
- [28] T. Aaltonen *et al.* [CDF Collaboration], *Phys. Rev. Lett.* **100**, 182002 (2008) [arXiv:0712.1506 [hep-ex]].

- [29] V.M. Abazov *et al.* [D0 Collaboration], *Phys. Rev. Lett.* **101**, 012001 (2008) [arXiv:0802.4258 [hep-ex]].
- [30] R. Aaij *et al.* [LHCb Collaboration], *Phys. Rev. Lett.* **109**, 232001 (2012) [arXiv:1209.5634 [hep-ex]]; **113**, 152003 (2014) [arXiv:1408.0971 [hep-ex]]; *Phys. Rev. D* **90**, 032009 (2014) [arXiv:1407.2126 [hep-ex]]; *Eur. Phys. J. C* **74**, 2839 (2014) [arXiv:1401.6932 [hep-ex]]; *Phys. Rev. Lett.* **111**, 181801 (2013) [arXiv:1308.4544 [hep-ex]]; *J. High Energy Phys.* **1309**, 075 (2013) [arXiv:1306.6723 [hep-ex]]; *Phys. Rev. D* **87**, 112012 (2013) [arXiv:1304.4530 [hep-ex]].
- [31] M. Karliner, J.L. Rosner, *Phys. Rev. D* **90**, 094007 (2014) [arXiv:1408.5877 [hep-ph]].
- [32] M. Karliner, H.J. Lipkin, arXiv:hep-ph/0307243; *Phys. Lett. B* **575**, 249 (2003).
- [33] M. Karliner, B. Keren-Zur, H.J. Lipkin, J.L. Rosner, arXiv:0706.2163 [hep-ph].
- [34] M. Karliner, B. Keren-Zur, H.J. Lipkin, J.L. Rosner, arXiv:0708.4027 [hep-ph]; *Ann. Phys.* **324**, 2 (2009) [arXiv:0804.1575 [hep-ph]].
- [35] K. Anikeev *et al.*, arXiv:hep-ph/0201071.
- [36] V.V. Kiselev, A.K. Likhoded, *Phys. Usp.* **45**, 455 (2002) [*Usp. Fiz. Nauk* **172**, 497 (2002)] [arXiv:hep-ph/0103169].
- [37] J.D. Bjorken, Fermilab preprint, *Estimates of Decay Branching Ratios for Hadrons Containing Charm and Bottom Quarks*, FERMILAB-PUB-86-189-T, <http://lss.fnal.gov/archive/1986/pub/fermilab-pub-86-189-t.pdf>
- [38] M.A. Moinester, *Z. Phys. A* **355**, 349 (1996) [arXiv:hep-ph/9506405].
- [39] N. Brambilla *et al.* [Quarkonium Working Group], arXiv:hep-ph/0412158.
- [40] C.H. Chang, X.G. Wu, *Eur. Phys. J. C* **38**, 267 (2004) [arXiv:hep-ph/0309121].
- [41] Y.N. Gao *et al.*, *Chin. Phys. Lett.* **27**, 061302 (2010).
- [42] Y. Amhis *et al.* [Heavy Flavor Averaging Group], arXiv:1207.1158 [hep-ex].
- [43] R. Aaij *et al.* [LHCb Collaboration], *Phys. Rev. D* **85**, 032008 (2012) [arXiv:1111.2357 [hep-ex]].
- [44] R. Aaij *et al.* [LHCb Collaboration], *J. High Energy Phys.* **1304**, 001 (2013) [arXiv:1301.5286 [hep-ex]].
- [45] LHCb Collaboration, LHCb-CONF-2013-011, presented at EPS Conference, Stockholm, 2013.
- [46] R. Aaij *et al.* [LHCb Collaboration], arXiv:1405.6842 [hep-ex].
- [47] Y. Kato *et al.* [Belle Collaboration], *Phys. Rev. D* **89**, 052003 (2014) [arXiv:1312.1026 [hep-ex]].

- [48] V.V. Kiselev, A.K. Likhoded, M.V. Shevlyagin, *Phys. Lett. B* **332**, 411 (1994) [arXiv:hep-ph/9408407].
- [49] J.P. Ma, Z.G. Si, *Phys. Lett. B* **568**, 135 (2003) [arXiv:hep-ph/0305079].
- [50] M. Karliner, M. Low, J.L. Rosner, L.T. Wang, *Phys. Rev. D* **92**, 035010 (2015) [arXiv:1503.07209 [hep-ph]].
- [51] A. Denig, *Nucl. Phys. Proc. Suppl.* **162**, 81 (2006) [arXiv:hep-ex/0611024].
- [52] W. Kluge, *Nucl. Phys. Proc. Suppl.* **181–182**, 280 (2008) [arXiv:0805.4708 [hep-ex]].
- [53] H. Czyz, A. Grzelinska, J.H. Kuhn, *Phys. Rev. D* **81**, 094014 (2010) [arXiv:1002.0279 [hep-ph]].
- [54] V.P. Druzhinin, S.I. Eidelman, S.I. Serednyakov, E.P. Solodov, *Rev. Mod. Phys.* **83**, 1545 (2011) [arXiv:1105.4975 [hep-ex]].
- [55] See <http://cern.ch/fcc-ee>
- [56] See <http://cepc.ihep.ac.cn>; *Physics World*, Aug. 26, 2014.
- [57] For a discussion of this possibility see M. Ruan, arXiv:1411.5606 [hep-ex].
- [58] CEPC-SPPC Preliminary Conceptual Design Report, to appear.
- [59] M. Bicer *et al.* [TLEP Design Study Working Group], *J. High Energy Phys.* **1401**, 164 (2014) [arXiv:1308.6176 [hep-ex]].
- [60] K.A. Olive *et al.* [Particle Data Group], *Chin. Phys. C* **38**, 090001 (2014).
- [61] R.M. Barnett *et al.* [Particle Data Group], *Phys. Rev. D* **54**, 1 (1996).
- [62] C. Biscari, arXiv:physics/0401031.
- [63] M.S. Chen, P.M. Zerwas, *Phys. Rev. D* **12**, 187 (1975).
- [64] M.S. Chen, P.M. Zerwas, *Phys. Rev. D* **11**, 58 (1975).
- [65] D. Curtin, R. Essig, S. Gori, J. Shelton, arXiv:1412.0018 [hep-ph].
- [66] B. Aubert *et al.* [BaBar Collaboration], *Phys. Rev. Lett.* **90**, 242001 (2003) [arXiv:hep-ex/0304021].
- [67] D. Besson *et al.* [CLEO Collaboration], *Phys. Rev. D* **68**, 032002 (2003) [*Erratum ibid.* **75**, 119908 (2007)] [arXiv:hep-ex/0305100].
- [68] K. Abe *et al.* [Belle Collaboration], *Phys. Rev. Lett.* **92**, 012002 (2004).
- [69] W.A. Bardeen, E.J. Eichten, C.T. Hill, *Phys. Rev. D* **68**, 054024 (2003) [arXiv:hep-ph/0305049].
- [70] M.A. Nowak, M. Rho, I. Zahed, *Acta Phys. Pol. B* **35**, 2377 (2004) [arXiv:hep-ph/0307102].